International Journal of Heat and Mass Transfer 93 (2016) 250–256

Contents lists available at ScienceDirect

International Journal of Heat and Mass Transfer

journal homepage: www.elsevier.com/locate/ijhmt

A particle swarm approach for optimization of secondary cooling process in slab continuous casting

Xudong Wang [a,*], Zhaofeng Wang [b], Yu Liu [a], Fengming Du [a], Man Yao [a], Xiaobing Zhang [c]

[a] School of Materials Science and Engineering, Dalian University of Technology, Dalian 116024, China
[b] College of Information Science and Technology, Bohai University, Jinzhou City 12101, China
[c] Chief Engineer Office, Jiangsu Shagang Group, Zhangjiagang 21562, China

ARTICLE INFO

Article history:
Received 7 April 2015
Received in revised form 11 October 2015
Accepted 12 October 2015
Available online 22 October 2015

Keywords:
Secondary cooling
Heat transfer
Particle swarm optimization
Continuous casting

ABSTRACT

Secondary cooling control is the key factor for stabilizing and enhancing slab quality in continuous casting. In view of practical importance of critical boundary conditions in offline or online simulation and control during continuous casting process, accurate estimation for heat transfer coefficient of secondary cooling zone is of utmost significance. To optimize the cooling process and temperature behavior of continuous casting slab, a novel method was presented to predict the heat transfer behavior in secondary cooling process. This approach applies the particle swarm optimization (PSO) algorithm in conjunction with the mathematical heat transfer model and the experimental temperature to determine the heat transfer coefficient. Through verifying the validity and efficiency of the integrated method proposed, the temperature variation of slab surface is more coincident with measured temperatures along the casting direction. The calculation results confirm that the heat transfer coefficient could be estimated precisely with measurement temperatures using PSO algorithm. The combined approach offers an applicable technology for optimization of cooling strategy and solidifying process in continuous casting.

1. Introduction

Continuous casting is currently the primary method of producing steel slabs, billets and blooms. Heat transfer plays an important role in productivity and quality of steel prior to rolling. Various kinds of surface and internal quality defects originate from improper cooling practices [1,2]. Accurate description of heat transfer and reasonable control of secondary cooling process are the basic requirements for high efficient continuous casting. For the sake of competitiveness in manufacturing, there is a permanent requirement of proper cooling strategies in the secondary cooling areas to obtain excellent product quality.

Zone different casting speed are listed in Table 4. Many heat transfer models have been developed and successfully used to simulate steady state casting operations in online or offline mode. In terms of process control, this means a necessity to maintain operational parameters in a specific optimum range. Owing to the complicated and economic reasons, it is not feasible to undertake extensive experimental trials during the continuous casting process to evaluate the influence of several operational parameters. In this sense, the rapid development of better process control and optimization is increasingly dependent on simulations performed with heat transfer mathematical models and artificial intelligence techniques [3–5].

Aiming to enhancing internal quality of casting slab, the accurate prediction of surface temperature and solidifying state of strands are obviously essential and strongly dependent on the boundary conditions of heat flux, especially for the heat transfer coefficient in each secondary cooling zone. In the present work, this paper presents a mathematical heat transfer model combined with the particle swarm optimization (PSO) to optimize the secondary cooling process. The heat transfer model is built and uses a two-dimensional finite difference method to calculate the thermal field and the solid shell profile. The PSO algorithm is applied to find the optimal heat transfer coefficient in each secondary cooling zone for the production of slabs with a better temperature dropping trend. Improved calculation conditions of the new configuration are compared to the original one. The accuracy and efficiency of the integrated approach is investigated further.

2. Description of the mathematical model

The numerical modeling of the strand has been developed to track a transverse slice of a steel slab as it moves down along the casting direction. Model is based on the finite difference method.

* Corresponding author. Tel.: +86 0411 84707347.
E-mail address: hler@dlut.edu.cn (X. Wang).

http://dx.doi.org/10.1016/j.ijheatmasstransfer.2015.10.025
0017-9310/

In view of the geometric features of the slab, the temperature profile only needed to be calculated for one quarter of slab cross-section as shown in Fig. 1.

2.1. Assumptions

The following assumptions were made in the formulating of the model:

(a) Heat transfer along the direction of slab width and thickness is recognized as axial symmetry and that along the slab withdrawal direction is neglected. Therefore, the mathematical model is translated into a two-dimensional unsteady heat conduction equation.
(b) The latent heat of steel solidification is converted into an equivalent specific heat capacity in the mushy zone (semisolid zone).
(c) The density of steel is constant, but the specific heat capacity and the heat conductivity of steel are the temperature-dependent properties.
(d) The fluid flow is expected to affect thermal field via enhanced heat transfer and then an effective thermal conductivity is employed in the liquid core and mushy zone of slab.

2.2. Governing equations

According to above assumptions, a two-dimensional heat transfer equation is available as follows:

$$\rho c\frac{\partial T(x,y,t)}{\partial t}=\frac{\partial}{\partial x}\left(\lambda\frac{\partial T(x,y,t)}{\partial x}\right)+\frac{\partial}{\partial y}\left(\lambda\frac{\partial T(x,y,t)}{\partial y}\right)+S \quad (1)$$

where ρ is steel density, kg m^{-3}; c is specific heat of steel, J kg^{-1} K^{-1}; T represents the instaneous slab temperature, K; t is time, s; λ is thermal conductivity, W m^{-1} K^{-1}; x and y are coordinates, m, and represent the direction of slab width and slab thickness; S is energy source term, W m^{-3}.

The equivalent specific heat method is adopted to calculate the latent heat of steel, which transforms the influence of latent heat to specific heat. The formula is expressed as follows proposed by Thomas [2]:

$$C_{eff}=C_p+\frac{L_H}{T_l-T_s}(T_s\leqslant T\leqslant T_l) \quad (2)$$

where C_{eff} represents equivalent specific heat, J kg^{-1} K^{-1}; C_p represents the specific heat of steel; L_H is the latent heat of solidification, J kg; T_l represents the liquidus temperature of steel, K; T_s represents the solidus temperature of steel, K.

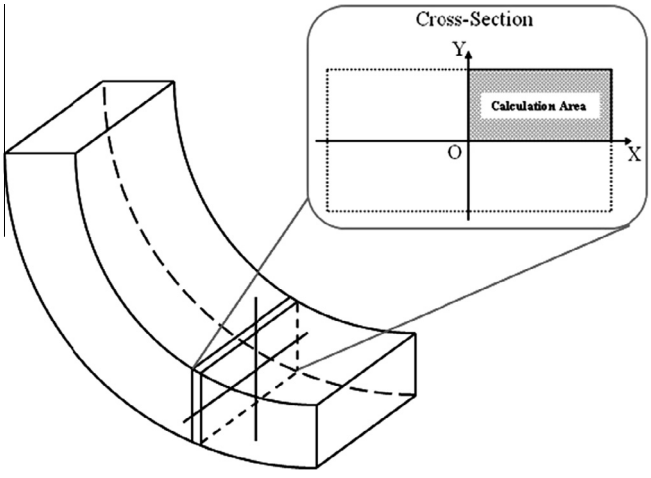

Fig. 1. Schematic diagram of the calculation domain.

Table 1
Overview of each secondary cooling zone for the caster.

Secondary cooling zone	1#	2#	3#	4#	5#	6#	7#	8#
Distance from meniscus (m)	0.8	1.04	1.97	3.34	5.26	9.10	12.94	19.65
Length (m)	0.24	0.93	1.37	1.92	3.84	3.84	6.71	9.69

In the temperature between T_l and T_s, the convection effect of the mushy zone kinetics on heat transfer is not known. The thermal conductivity is given as [3]:

$$\lambda_{eff}=\lambda_{sol}(1+6f_l) \quad (3)$$

where λ_{sol} is thermal conductivity of solid steel, f_l is the liquid fraction.

2.3. Initial and boundary conditions

At the beginning of the continuous casting ($t = 0$), the slice temperature profile at the meniscus is equal to the pouring temperature:

$$T(x,y,t)|_{t=0}=T_{cast} \quad (4)$$

where T_{cast} is the casting temperature, K, which is measured in tundish.

The boundary conditions are as follows:

In the mold, an average heat flux as a function of the casting time is utilized and the boundary heat flux is described by Savage and Pritchard [1]:

$$Q=A-B\sqrt{\frac{z}{V_{cast}}} \quad (5)$$

where Q represents the mold heat flux, W m^2; A and B are the coefficients relative to heat flux in the mold; z is the distance from meniscus, m; V_{cast} is casting speed, m min.

The heat transfer coefficient in the spray zones is usually related to spray water flow rates, and can be calculated through the formula (6) [4]:

$$h_{spray}=\frac{1570.0w^{0.55}[1.0-0.0075(T_{spray}-273.15)]}{\alpha} \quad (6)$$

where w is the spray cooling flux, L m^{-2} s^{-1}; T_{spray} represents the temperature of the spray cooling water, K; α is a machine dependent calibration factor; h_{spray} represents the spray cooling heat transfer coefficient, W m^{-2} K^{-1}.

A Newtonian heat-transfer coefficient is then used to compute radiation heat transfer between the slab and surrounding environment as described by Hardin et al. [5]:

Table 2
Casting conditions and thermo-physical properties.

Item	Symbol	Value	Unit
Slab section	$W \times N$	2450 × 320	mm × mm
Effective mold length	L_{mold}	800	mm
Carbon content	C%	0.12	%
Pouring temperature	T_{cast}	1544.0	°C
Steel liquidus temperature	T_l	1514.4	°C
Steel solidus temperature	T_s	1453.3	°C
Casting speed	V_{cast}	0.65	m/min
Steel density	ρ	7200	kg/m^3
Latent heat	L_h	2.7−E5	J/kg
Spray water temperature	T_{spray}	30.0	°C
Ambient temperature	$T_{ambient}$	35.0	°C

Table 3
Major components of steel grades.

[%C]	[%Si]	[%Mn]	[%P]	[%S]	[%Cr]	[%Al]	[%N]
0.12	0.3	1.5	0.024	0.01	0.08	0.04	0.0048

Table 4
Water volume of each secondary cooling zone at a casting speed of 0.65 m/min.

Secondary cooling zone	1#	2#	3#	4#	5#	6#	7#	8#
Water volume (L/min)	182	368	245	47	50	35	61	85

$$h_{rad} = \varepsilon\sigma(T_{surface}^2 + T_{ambient}^2)(T_{surface} + T_{ambient}) \quad (7)$$

where ε is the emissivity of slab surface; σ is the Stefan–Boltzmann constant, 5.6684×10^{-8} W m^{-2} K^{-4}; $T_{surface}$ represents the slab surface temperature, K; $T_{ambient}$ represents the ambient temperature, K.

2.4. Experimental conditions

Based on the equations mentioned above, a heat transfer calculation model was developed with finite difference method (FDM).The model is used to predict the temperature and shell thickness distributions in a slab continuous caster. The bow-type caster is used to produce 220/320 mm thick slab in a width of 1800–2700 mm. The corresponding highest casting speed of the two kinds of sections is 1.2 m min^{-1} and 0.8 m min^{-1}, respectively. The caster radius is 10.75 m and the metallurgical length is 28.83 m. Effective mold length is 800 mm. The caster has 8 secondary cooling zones, and the distance below the meniscus and the length of each secondary cooling zone are given in Table 1. The principal simulation parameters and thermo-physical properties are shown in Tables 2 and 3. Here, # means the zone numbers of each secondary cooling zone.

To investigate the declining trend of the slab surface temperature, the centerline temperature of broader face on slab surface is continuously detected by applying non-contact infrared temperature sensors, at the 4#, 5#, 6#, 7# and 8# zone exits. To reduce the influence of vapor and oxide layer, the maximal value was extracted as the measured results during the stable casting state. The water volume of each secondary cooling zone and the measured temperature on slab surface at each measuring points under a casting speed of 0.65 m min^{-1} are listed in Tables 4 and 5.

3. Optimization for heat transfer coefficient

Usually, the heat transfer coefficient could be estimated from the conventional empirical formula (6) proposed by Nozaki [4]. However, the uncertain heat transfer coefficients have been severely affected by the hot temperature on slab surface, spraying nozzle, cooling length, water volume, nozzle status and so on. It is of importance for determination of the heat transfer coefficient under certain conditions in real casting process. Commonly, the direct heat conduction problems consist of determining the temperature distribution of the heated medium when the boundary and initial conditions, heat source, thermo-physical properties and geometric parameters are known. In contrast, the inverse heat conduction problems consider the identification of boundary or initial conditions, heat source, thermo-physical properties or geometric parameters by using the temperature measurements obtained at some specific locations in the medium. Using temperature measurements to determine boundary conditions is a common inverse heat conduction problem.

In the previous work, the model of inverse heat transfer problem (IHTP) was proposed to inversely simulate the heat transfer coefficients from the measured temperatures in a steel plant [6]. However, it was well known that the IHTP models were often regarded as the ill-posed problem because their solution did not satisfy the general requirements of existence, uniqueness and stability under small changes to the input data. In other words, their solutions need huge iterations, more time consuming, even unable to find convergence solutions and very sensitive to the measured data with measurement errors, measurement location and initial situations and so on. To overcome the limitations of IHTP models, this work propose an intelligent learning algorithms to the modeling for convenient estimation of the heat transfer coefficients.

3.1. Principle of the particle swarm optimization algorithm

Particle swarm optimization (PSO) is a high performance algorithm created as an alternative to genetic algorithm. The algorithm is an adaptive and robust parameter searching technique based on the conceptual model of bird foraging [7]. It is indeed a population-based stochastic algorithm which belongs to the evolutionary computation (EC) techniques. The main difference between the PSO and EC algorithms is that the PSO algorithm stores information about both its position and its velocity (change in position). However, the PSO finds the optimum value more quickly than traditional evolutionary algorithm. It is due to the fact that PSO uses a combination of local and global searches with the sharing evolutionary information among the individual particles.

In a PSO system with M particles, each individual is treated as a volume-less particle in the n-dimensional search space, with the position vector and velocity vector of particle i at the kth iteration. For the PSO algorithm, the searching procedure based on this concept can be described by:

$$v_i^{k+1} = w \cdot v_i^k + c_1 r_1 (p_i^k - x_i^k) + c_2 r_2 (p_g^k - x_i^k) \quad (8)$$

$$x_i^{k+1} = x_i^k + v_i^{k+1} \quad (9)$$

$x_i = \{x_{i1}, x_{i2}, \ldots, x_{in}\}^T$ is the position of the ith particle. $p_i = \{p_{i1}, p_{i2}, \ldots, p_{in}\}^T$ represents the best solution (*fitness*) of the ith particle has achieved so far (*pbest*); $p_g = \{p_{g1}, p_{g2}, \ldots, p_{gn}\}^T$

Table 5
Comparison of heat transfer calculation results between original and optimized by PSO algorithm.

Secondary cooling zone	Water volume (L/min)	Measured temperature (°C)	Results of formula (6)			PSO algorithm optimized		
			h_{spray} (W/m^2 K)	Calculated temperature (°C)	Error (°C)	h_{spray} (W/m^2 K)	Calculated temperature (°C)	Error (°C)
4#	47	965.2	82.5	1021.6	56.4	129.0	963.3	−1.9
5#	50	957.3	58.3	999.2	41.9	82.9	953.2	−4.1
6#	35	941.9	47.9	975.1	33.2	61.0	943.0	1.1
7#	61	915.5	47.8	927.2	11.7	52.2	910.6	−4.9
8#	85	890.7	46.9	916.1	25.4	63.0	890.4	−0.3
RMS					37.1			3.0

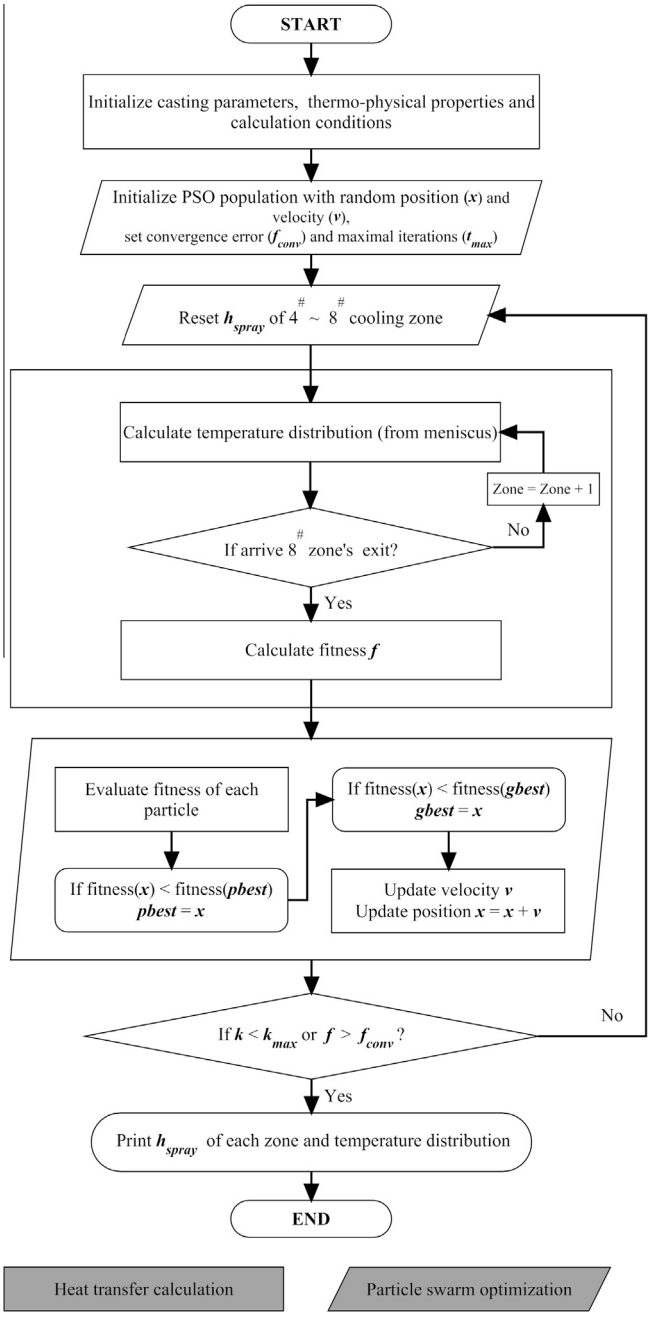

Fig. 2. Flowchart of the optimization process.

represents the overall best location obtained so far by all particles in the population (*gbest*). $v_i = \{v_{i1}, v_{i2}, \ldots, v_{in}\}^T$ expresses the velocity of the *i*th particle in the range of $|-v_i^{max}, v_i^{max}|$. v_i^{max} determines the resolution, or fitness, with which regions between the present position and target position are searched. n is the dimensions (number of optimization variables) of each particle. k is the number of iterations. $i = 1, 2, \ldots, M$, M is the particle swarm size of PSO.

where, w is the inertia factor. The constants c_1 and c_2 represent are the acceleration coefficient that pull each particle toward *pbest* and *gbest* positions. According to past experience, v_i^{max} is often set at 10–50% of the dynamic range of the variable on each dimension, and w, c_1, c_2 are often set to 0.8, 2, and 2, respectively [8,9]. r_1 and r_2 are uniform random variables in the range [0,1], are that pull each particle toward the local and the global best positions.

3.2. Design of fitness function

For an optimization problem, a proper fitness function plays a very important role in finding the optimum solution. In this work, problems in estimating unknown heat transfer coefficients are solved by minimizing the objective function, which is the root mean square (RMS) between the calculated and measured temperatures of slab surface at each secondary cooling zone. Thus, the fitness function can be defined as:

$$f = \sqrt{\frac{1}{N}\sum_{j=1}^{N}(T_C^j - T_M^j)^2} \tag{10}$$

where, T_C^i represents calculated value of the slab temperature and T_M^i is the measured value of the slab temperature. Combining with the later part of plant trial, T^i here represents the surface center temperature at the exits of 4th, 5th, 6th, 7th and 8th zone. N is the number of measured position, in other words, N is the number of optimization variables and equal to the particle's dimensions (n). Obviously, the task of this study is to estimate the heat transfer coefficient from measured surface temperatures of the 4#, 5#, 6#, 7# and 8# secondary cooling zone, therefore, the number of dimensions (n) of each particle is 5.

3.3. Computation procedure for the PSO

Owing to the difficulty of performing measurement at the exit of zones 1–3 in the secondary cooling zone, the values of heat transfer coefficient in these zones are substituted by the results of experiential formula [6]. Thus, the following contents of this work apply the PSO to estimate the heat transfer coefficients at zones 4–8. The computational steps of the PSO algorithm described above are given as follows:

```
Initialize calculation parameters of heat transfer model;
Initialize particles with random positions (x_i) and velocities (v_i);
Initialize pbest (p_i), gbest (p_g), inertia factor (w) and
  acceleration coefficient (c_1 and c_2), k = 0;
While (k < k_max) or (f > f_conv)
  Calculate the temperature field of slab slice;
  Update velocity of all particles according to Eq. (8);
  Update position of all particles according to Eq. (9);
  Apply velocity limits (v_i^max) to velocities;
  Evaluate all the particle's fitness (f_i), i = 1, 2, ..., M according
  to Eq. (8);
  Update pbest (p_i) and gbest (p_g);
  Update iterations k = k + 1;
End while
Output the final optimum gbest (p_g) as the estimated heat
  transfer coefficient.
```

At the beginning of PSO optimization, in order to give some idea on the range of searching space for PSO, the upper and lower limits of each dimension for all particles are set as 0.5 times and 2.0 times of the original heat transfer coefficients at zones 4–8, which are preliminarily determined through the experiential formula [6] and corresponding water volume, as shown in Table 4. In the following contents, PSO are adopted to optimize the cooling strategy of continuous casting slab.

If the maximum number of generation set k is reached the given number of iterations k_{max} or global best fitness f is lower than error limit f_{conv}, the optimization process would be ceased. According to the given fitness functions, calculate the fitness in every iteration

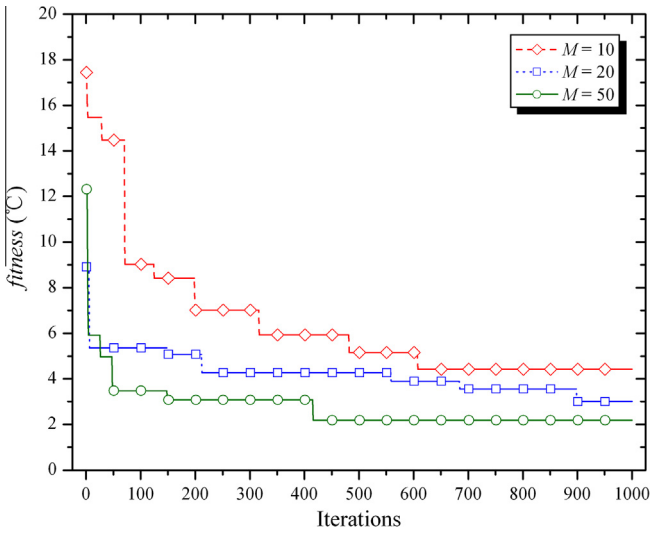

Fig. 3. Fitness function variation of the PSO algorithm with different swarm sizes.

combined with the results of heat transfer model during the optimization process, to achieve the minimum value of cost function through optimizing iteration, thus definite the rational heat transfer coefficient in each secondary cooling zone. The implementation of the standard PSO approach and heat transfer calculation for optimizing process can be carried out according to the flowchart presented in Fig. 2.

4. Results and discussion

4.1. Convergence of PSO algorithm

As a stochastic algorithm, whether or not to find a global minimum depends mainly on how to update a population. In theory, if a population can keep changing all the way, it has the ability to find the global minimum but in an infinite time. However, to make a stochastic algorithm efficient, strategies have to be proposed to reduce the large amount of time. As the number of iterations is fixed, the rapid convergence rate is necessary in practice.

First of all, the influences of swarm size on the convergence of fitness function for PSO are examined. Fig. 3 shows the optimization curve of PSO during iterative search process with the different swarm size. On the whole, in the earlier stage of search process of function optimization, the fitness objective function converges faster, but the convergence speed reduces gradually as the increasing iterations. It is clear to see that the fitness decreases more quickly with the increase of the size of particle swarm in the same iteration number. The swarm size of 50 shows faster convergence and smaller fitness which is about 2.2 °C after 1000 iterations. It should be noted that the computing time is measured for three population sizes, such as 10, 20, and 50, after 1000 iterations. As a result, increase in computing time is directly proportional to the swarm size. Thus, considering the best fitness, computational time and convergence speed of different swarm size synthetically, population size M is suggested to be 20.

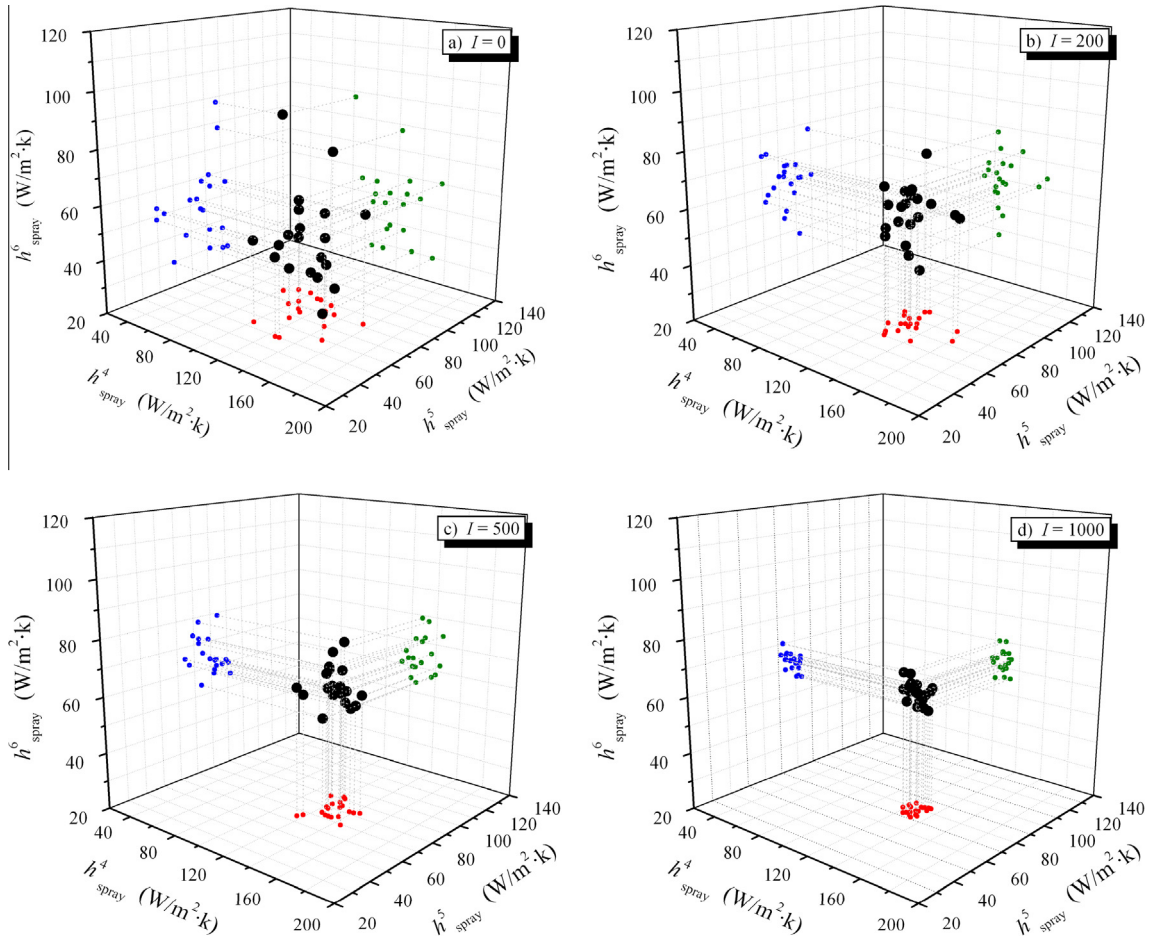

Fig. 4. Behavior of particle convergence at different iterations of a swarm size of 20.

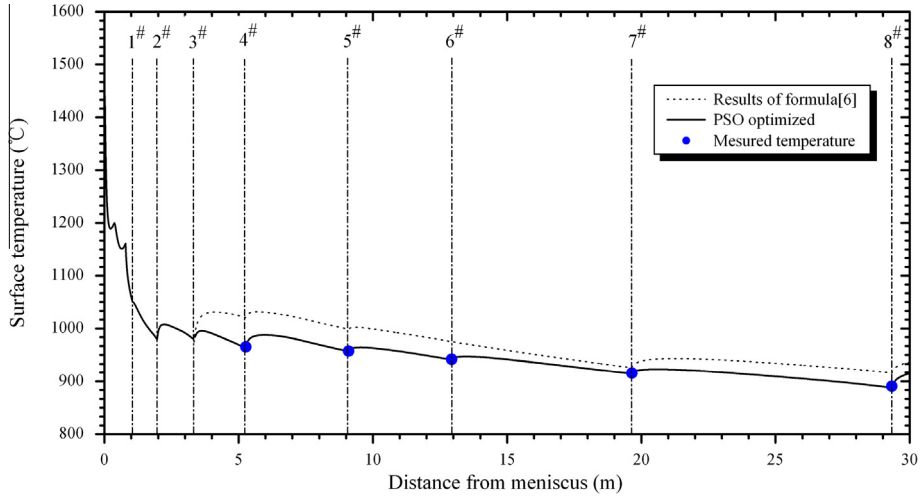

Fig. 5. Comparison between before and after optimization of surface temperature with the casting speed of 0.65 m/min.

Table 6
Comparison of heat transfer calculation results of shell thickness with experimental results.

Outlet of segment	Distance from meniscus (m)	Measured shell thickness (mm)	Calculated shell thickness (mm)	
			Results of formula (6)	PSO algorithm optimized
Seg. 7	16.93	122.5	119.7	121.7
Seg. 8	19.31	128.0	126.5	127.8
Seg. 9	21.70	133.5	132.3	133.9

4.2. Estimation of heat transfer coefficients

20 Particles are deployed to search for the location of heat transfer coefficients for the $4^{\#}$, $5^{\#}$, $6^{\#}$, $7^{\#}$ and $8^{\#}$ secondary cooling zone. To illustrate the movement of all particles, the convergence behavior of h^4_{spray}, h^5_{spray} and h^6_{spray} is shown in Fig. 4. Figures show the movement of particles for each iteration when searching the actual location of heat transfer coefficients. The particles are randomly distributed in the searching region for the first iteration. After the 200 iterations, the particles are starting to make a cluster and some particles have a relatively smaller fitness. However, the cost functions of several particles are still greater than 5.0 °C. It might because of the use of constant weight inertia that hinders the movement of particles for higher iteration. On the subsequent iterations, each particle tends to move towards the actual heat transfer coefficients as shown in Fig. 4(c). In this condition, the actual heat transfer coefficients have been detected by some particles that have the cost function as shown in Fig. 3. By further increasing the iterations to 1000, the clustering becomes dense which means that the heat transfer coefficients have been determined by almost all particles, as given in Fig. 4(d). The best fitness of all particles is 3.0 °C, thus, the locations of the heat transfer coefficients have been identified, and optimum value of h^4_{spray}, h^5_{spray}, h^6_{spray}, h^7_{spray} and h^8_{spray} are 129.0, 82.9, 61.0, 52.2 and 63.0 W/m^2 K, respectively, as shown in Table 5. It shows that the proposed model can detect the heat transfer coefficients from the measured temperature. In addition, it should be pointed that the optimized heat transfer coefficients are usually larger than the values of empirical formula estimation, which means that the actual cooling effect is more intense than the effect of the formula calculation.

4.3. Heat transfer calculation results

The heat transfer coefficient of $4^{\#} \sim 8^{\#}$ cooling zone obtained formula (6) and their optimized value optimized by PSO are input into the heat transfer model, and the temperature distribution of slab slice along the casting direction are calculated respectively. The slab surface temperature profiles of wide face center before and after optimization are shown in Fig. 5. The slab surface temperature at each zone exit, the measured temperature and the temperature deviations before and after PSO optimization are compared as shown in Table 5. After PSO optimization, the slab surface temperature is further closer to objective temperature, the average temperature deviations between calculated slab surface and measured temperature at each zone exit decreases from 33.7 °C to 2.5 °C. The root mean square between surface temperature and target temperature decreases from 37.1 °C to 3.0 °C. The distributions of slab surface temperature are more rational, and it effectively improves the slab surface temperature variations along the casting direction which is beneficial to guarantee the quality of slab and meet the rolling requirements.

The pin-shooting experiment was also conducted under the same casting parameters, and the center points along the width direction at 7th, 8th and 9th segment exits were chosen as shooting positions respectively. The sulfur print and macro etching test are used in the experiment. The calculated results from heat transfer calculation model and measured shell thickness at each detecting position are given in Table 6. It can be seen that the calculated shell thickness obtained from formula (6) is always lower than the measured ones, and the maximal difference between them is 2.8 mm, which is located at the outlet of Seg. 7. The calculated shell thickness optimized by PSO algorithm coincides well as the measured data and has a maximum deviation of 0.8 mm. On the whole, the consistency between calculated results optimized by PSO algorithm and measured solidified shell thickness demonstrates the rationality and accuracy of the proposed model.

5. Conclusions

The optimum control of internal quality of the continuous casting slab is extremely dependent on the accurate selection of the heat transfer coefficient. In order to overcome the limitations of the method of inverse heat transfer problem, this paper presents a novel secondary cooling strategy optimization method based on particle swarm optimization. The PSO algorithm merged with

heat transfer calculation model is implemented to optimize the heat transfer coefficients of the secondary cooling zone from the knowledge of temperature measurements obtained on the slab surface. The results show that PSO algorithm converges fast and possesses strong global search ability and higher optimization efficiency. The root mean square between slab surface temperature and measured temperature at each zone exit decreases from 37.1 °C to 3.0 °C, which effectively decreases the temperature deviation as well as improves the slab surface temperature variation along the casting direction. The comparison of calculated shell thickness with pin-shooting experimental results also shows the accuracy of the proposed model. The computing results confirm that the PSO algorithm is remarkably good for accurate prediction of the heat transfer coefficients, especially in the case of the inverse estimation for boundary conditions in heat transfer calculation. Application of this algorithm may be used to solve other similar inverse problems, and it is also expected that the prediction accuracy of the proposed model will be further improved when more data are available in the future work.

Conflict of interest

None declared.

Acknowledgments

We would like to acknowledge the financial support of the National Natural Science Foundation of China (51004012/51474047). This Project was granted financial support from China Postdoctoral Science Foundation (2012M520621/2013T60511). Also, the supports of the Fundamental Research Funds for the Central Universities and the Key Laboratory of Solidification Control and Digital Preparation Technology (Liaoning Province) are gratefully acknowledged.

References

[1] J. Savage, W.H. Pritchard, Problem of rupture of the billet in the continuous casting of steel, Iron Steel Inst. 178 (11) (1954) 269–277.
[2] B.G. Thomas, I.V. Samarasekera, J.K. Brimacombe, Comparison of numerical modeling techniques for complex, two-dimensional, transient heat-conduction problems, Metall. Mater. Trans. B 15 (2) (1984) 307–318.
[3] J.S. Ha, J.R. Cho, B.Y. Lee, M.Y. Ha, Numerical analysis of secondary cooling and bulging in the continuous casting of slabs, J. Mater. Processing Technol. 113 (1–3) (2001) 257–261.
[4] T. Nozaki, J. Matsuno, K. Murata, H. Ooi, M. Kodama, Secondary cooling pattern for preventing surface cracks of continuous casting slab, Trans. ISIJ 18 (6) (1978) 330–338.
[5] R.A. Hardin, K. Liu, A. Kapoor, C.A. Beckermann, Transient simulation and dynamic spray cooling control model for continuous steel casting, Metall. Mater. Trans. B 34B (3) (2003) 297–306.
[6] Z.F. Wang, M. Yao, X.D. Wang, X.B. Zhang, L.S. Yang, H.Z. Lu, X. Wang, Inverse problem-coupled heat transfer model for steel continuous casting, J. Mater. Process. Technol. 214 (2014) 44–49.
[7] J. Kennedy, R. Eberhart, Proceedings of the IEEE International Conference on Neural Networks, IEEE Service Center, Piscataway, NJ, Perth, Australia, 1995 (pp. 1942–1945).
[8] R. Perez, K. Behdinan, Particle swarm approach for structural design optimization, Comput. Struct. 85 (13–14) (2007) 1579–1588.
[9] D. Marco, B. Christian, Ant colony optimization theory: a survey, Theoret. Comput. Sci. 344 (2–3) (2005) 243–278.